Open access • Journal Article • DOI:10.1109/TEMC.2010.2051949

Guaranteed Passive Parameterized Model Order Reduction of the Partial Element Equivalent Circuit (PEEC) Method — Source link

Francesco Ferranti, Giulio Antonini, Tom Dhaene, Luc Knockaert

Institutions: Ghent University, University of L'Aquila

Published on: 16 Sep 2010 - IEEE Transactions on Electromagnetic Compatibility (IEEE)

Topics: Partial element equivalent circuit, Equivalent circuit, Model order reduction, Parametric statistics and Electronic circuit

Guaranteed Passive Parameterized Model Order Reduction of the Partial Element Equivalent Circuit (PEEC) Method

Francesco Ferranti, *Member, IEEE*, Giulio Antonini, *Senior Member, IEEE*, Tom Dhaene, *Senior Member, IEEE*, and Luc Knockaert, *Senior Member, IEEE*

***Abstract*—The decrease of IC feature size and the increase of operating frequencies require 3-D electromagnetic methods, such as the Partial Element Equivalent Circuit (PEEC) method, for the analysis and design of high-speed circuits. Very large systems of equations are often produced by 3-D electromagnetic methods. During the circuit synthesis of large scale digital or analog applications, it is important to predict the response of the system under study as a function of design parameters, such as geometrical and substrate features, in addition to frequency (or time). Parameterized model order reduction (PMOR) methods become necessary to reduce large systems of equations with respect to frequency and other design parameters.**

We propose an innovative PMOR technique applicable to PEEC analysis, which combines traditional passivity-preserving model order reduction methods and positive interpolation schemes. It is able to provide parametric reduced order models, stable and passive by construction over a user defined range of design parameter values. Numerical examples validate the proposed approach.

***Index Terms*—Partial Element Equivalent Circuit method (PEEC), parameterized model order reduction (PMOR), interpolation, passivity.**

I. Introduction

Electromagnetic (EM) methods [1]–[3] have become increasingly indispensable analysis and design tools for a variety of complex high-speed systems. Users are usually only interested in a few field (*E,H*) or circuit (*i,v*) unknowns at the input and output ports, in the frequency domain or time domain, while the use of these methods usually results in the computation of a huge number of field or circuit unknowns. Therefore, model order reduction (MOR) techniques are crucial to reduce the complexity of EM models and the computational cost of the simulations, while retaining the important physical features of the original system [4]–[8]. The development of a reduced order model (ROM) of the EM system has become a topic of intense research over the last years. Important applications of EM-based modeling include high-speed packages, interconnects, vias, and on-chip passive components [9]–[11]. Among EM methods, the Partial Element Equivalent Circuit (PEEC) method has gained an increasing popularity among electromagnetic compatibility engineers due to its capability to transform the EM system under examination into a passive RLC equivalent circuit. PEEC uses a circuit interpretation of the electric field integral equation (EFIE), thus allowing to handle complex problems involving EM fields and circuits [2], [12]. The PEEC equivalent circuits are usually connected with nonlinear circuit devices such as drivers and receivers in a time domain circuit simulator (e.g. SPICE). However, inclusion of the PEEC model directly into a circuit simulator may be computationally intractable for complex structures, because the number of circuit elements can be in the tens of thousands. For this reason, MOR techniques are often used to reduce the size of a PEEC model [8], [13]. A passive reduced-order interconnect macromodeling algorithm, known as PRIMA [8], has received great attention due to its capability to generate passive models of RLC circuits, which is important because stable, but nonpassive models can produce unstable systems when connected to other stable, even passive, loads.

Traditional MOR techniques perform model reduction only with respect to frequency. However, during the circuit synthesis of large scale digital or analog applications, it is also important to predict the response of the circuit under study as a function of environmental effects, manufacturing variations, and fluctuations in the critical dimensions of transmission lines such as width and height. Typical design process includes optimization and design space exploration, and thus requires repeated simulations for different design parameter values. It is often not feasible to perform multiple simulations of large circuits due to variations in these parameters. Such design activities call for parameterized model order reduction (PMOR) methods that can reduce large systems of equations with respect to frequency and other design parameters of the circuit, such as geometrical layout or substrate characteristics.

A number of PMOR methods have been developed. The perturbation technique [14] is one of the early work to capture small variation around the nominal circuit values. Other PMOR techniques are based on statistical performance analysis [15], [16]. Multiparameter moment-matching methods presented in [17], [18] use a subspace projection approach and guarantee the passivity. However, the structure of such methods may present some computational problems, and the resulting reduced models usually suffer from oversize when

Manuscript received November 2009.

Francesco Ferranti, Tom Dhaene and Luc Knockaert are with the Department of Information Technology (INTEC), at Ghent University - IBBT, Sint Pietersnieuwstraat 41, 9000 Ghent, Belgium, email: {francesco.ferranti, tom.dhaene, luc.knockaert}@ugent.be.

Giulio Antonini is with the UAq EMC Laboratory, Dipartimento di Ingegneria Elettrica e dell'Informazione, Università degli Studi dell'Aquila, Via G. Gronchi 18, 67040, L'Aquila, Italy, e-mail: giulio.antonini@univaq.it.

This work was supported by the Research Foundation Flanders (FWO) and by the Italian Ministry of University (MIUR) under a Program for the Development of Research of National Interest, (PRIN grant n. 20089J4SM9-002).

the number of moments to match is high, either because high accuracy (order) is required or because the number of parameters is large. The Compact Order Reduction for parameterized Extraction (CORE) algorithm [19] is an explicit-and-implicit scheme. It is numerically stable, but unfortunately it does not preserve the passivity. The Parameterized Interconnect Macromodeling via a two-directional Arnoldi process (PIMTAP) algorithm presented in [20] is numerically stable, preserves the passivity of parameterized RLC networks, but, such as all multiparameter moment-matching based PMOR techniques, it is suitable only to a low-dimensional design space.

This paper proposes a PMOR method applicable to PEEC analysis that provides parametric reduced order models, stable and passive by construction over the design space of interest. It combines traditional passivity-preserving model order reduction methods and interpolation schemes based on a class of positive interpolation operators [21], to guarantee overall stability and passivity of the parametric reduced order model. A method has been recently proposed in [22], [23] based on an efficient and reliable combination of rational identification and positive interpolation schemes to build parameterized macromodels, stable and passive by construction over the design space of interest, starting from multivariate data samples of the input-output system behavior and not from system equations as in all PMOR techniques previously discussed. The PMOR method proposed in this paper starts by computing a set of reduced order PEEC models using the PRIMA algorithm for different design parameters values. The PEEC models are put into a state-space form for which PRIMA preserves passivity. The PEEC models and the corresponding reduced models obtained by means of PRIMA describe an admittance ($\mathbf{Y}$) representation. Since at microwave frequencies, the $\mathbf{Y}$-representation cannot be accurately measured, the scattering parameters ($\mathbf{S}$) representation is used to describe the broadband frequency behavior of microwave systems. Therefore, the reduced models are translated from $\mathbf{Y}$-representation into $\mathbf{S}$-representation. In the following paper we refer to these initial $\mathbf{S}$-reduced order models as *root ROMs*. However, it should be noted that the proposed PMOR technique is not bound to PRIMA, other passivity-preserving MOR methods can be used, such as the Laguerre-SVD MOR [24] or the passivity-preserving truncated balanced realization algorithms [25]. Finally, a parametric ROM is built by combining all *root ROMs* through an interpolation scheme that preserves stability and passivity properties over the complete design space.

The paper is organized as follows. Section II describes the modified nodal analysis (MNA) equations of the PEEC method. Section III describes the proposed PMOR method. Finally, some numerical examples are presented in Section IV, validating the proposed technique.

II. PEEC FORMULATION

The PEEC method [2] starts from the integral equation form of Maxwell's equations. It has received an increasing interest by electrical engineers since it provides a circuit interpretation of the EFIE equation, thus allowing to handle complex problems involving both circuits and electromagnetic fields [2], [12], [26]–[30]. In what follows, we describe a quasi-static PEEC formulation [2] that approximates the full-wave PEEC approach [26].

In the standard approach, volumes and surfaces of conductors and dielectrics are respectively discretized into hexahedra and patches that represent elementary regions [30] over which the current and charge densities are expanded into a series of basis functions. Pulse basis functions are usually adopted as expansion and weight functions. Such choice of pulse basis functions corresponds to assume constant current density and charge density over the elementary volume (inductive) and surface (capacitive) cells, respectively.

Following the standard Galerkin's testing procedure, topological elements, namely nodes and branches, are generated and electrical lumped elements are identified modeling both the magnetic and electric field coupling.

Conductor losses are modeled by their ohmic resistance, while dielectrics requires modeling the excess charge due to the dielectric polarization. This is done by means of the excess capacitance which is placed in series to the partial inductance of each dielectric elementary cell. Magnetic field coupling between elementary volume cells is characterized by partial inductances, while electric field coupling is modeled by the coefficients of potential. An example of PEEC circuit electrical quantities for a conductor elementary cell is illustrated, in the Laplace domain, in Fig. 1 where the current controlled voltage sources $sL_{p,ij}I_j$ and the current controlled current sources I_{cci} model the magnetic and electric field coupling, respectively. Hence, Kirchoff's laws for conductors can be re-written as

$$\mathbf{P}^{-1}\frac{d\mathbf{v}(t)}{dt} - \mathbf{A}^T\mathbf{i}(t) - \mathbf{i}_e(t) = \mathbf{0} \tag{1a}$$

$$-\mathbf{A}\mathbf{v}(t) - \mathbf{L}_p\frac{d\mathbf{i}(t)}{dt} - \mathbf{R}\mathbf{i}(t) = \mathbf{0} \tag{1b}$$

where $\mathbf{v}(t)$ denotes the node potentials to infinity, $\mathbf{i}(t)$ denotes the currents flowing in volume cells, $\mathbf{P}$ and $\mathbf{L}_p$ are the coefficients of potential and partial inductance matrices, respectively, $\mathbf{R}$ is a diagonal matrix containing the resistances of volume cells, $\mathbf{A}$ is the incidence matrix, $\mathbf{i}_e(t)$ represents the external currents. A selection matrix $\mathbf{K}$ is introduced to define the port voltages by selecting node potentials. The same matrix is used to obtain the external currents $\mathbf{i}_e(t)$ by the n_p port currents $\mathbf{i}_p(t)$

$$\mathbf{v}_p(t) = \mathbf{K}\mathbf{v}(t) \tag{2a}$$

$$\mathbf{i}_e(t) = -\mathbf{K}^T\mathbf{i}_p(t) \tag{2b}$$

When dielectrics are considered, the resistance voltage drop $\mathbf{R}\mathbf{i}(t)$ is substituted by the excess capacitance voltage drop that is related to the excess charge by $\mathbf{v}_d(t) = \mathbf{C}_d^{-1}\mathbf{q}_d(t)$ [31]. As a consequence, the polarization current flowing through the dielectric is modeled in terms of the excess voltage drop as well. Hence, for dielectric elementary volumes, equations (1)

become

$$\mathbf{P}^{-1}\frac{d\mathbf{v}(t)}{dt} - \mathbf{A}^T\mathbf{i}(t) - \mathbf{i}_e(t) = \mathbf{0} \tag{3a}$$

$$-\mathbf{A}\mathbf{v}(t) - \mathbf{L}_p\frac{d\mathbf{i}(t)}{dt} - \mathbf{v}_d(t) = \mathbf{0} \tag{3b}$$

$$\mathbf{i}(t) = \mathbf{C}_d\frac{d\mathbf{v}_d(t)}{dt} \tag{3c}$$

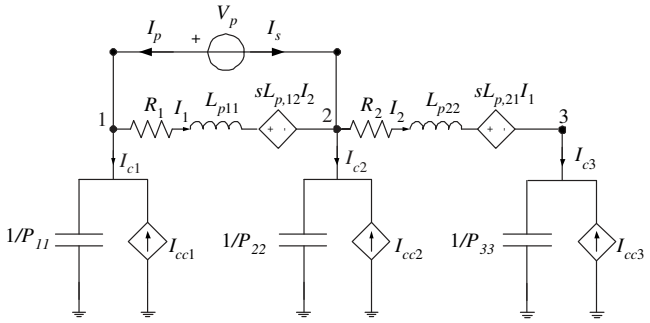

Fig. 1. Illustration of PEEC circuit electrical quantities for a conductor elementary cell.

A. Descriptor representation of PEEC circuits

Let us assume to have discretized the system under study consisting of conductors and dielectrics and to have generated n_i volume cells where currents flow and n_n surface cells where charge is located; the resultant number of elementary cells of conductors and dielectrics is n_c and n_d, respectively and that of electrical nodes is n_n. Furthermore, let us assume to be interested in generating an admittance representation $\mathbf{Y}(s)$ having n_p output currents $\mathbf{i}_p(t)$ under voltage excitation $\mathbf{v}_p(t)$. If the MNA approach [32] is used, the global number of unknowns is $n_u = n_i + n_d + n_n + n_p$. In a matrix form, the previous equations (1)-(3) read

$$\underbrace{\begin{bmatrix} \mathbf{P}^{-1} & \mathbf{0}_{n_n,n_i} & \mathbf{0}_{n_n,n_d} & \mathbf{0}_{n_n,n_p} \\ \mathbf{0}_{n_i,n_n} & \mathbf{L}_p & \mathbf{0}_{n_i,n_d} & \mathbf{0}_{n_i,n_p} \\ \mathbf{0}_{n_d,n_n} & \mathbf{0}_{n_d,n_i} & \mathbf{C}_d & \mathbf{0}_{n_d,n_p} \\ \mathbf{0}_{n_p,n_n} & \mathbf{0}_{n_p,n_i} & \mathbf{0}_{n_p,n_d} & \mathbf{0}_{n_p,n_p} \end{bmatrix}}_{\mathbf{C}} \frac{d}{dt} \underbrace{\begin{bmatrix} \mathbf{v}(t) \\ \mathbf{i}(t) \\ \mathbf{v}_d(t) \\ \mathbf{i}_p(t) \end{bmatrix}}_{\mathbf{x}(t)} =$$

$$-\underbrace{\begin{bmatrix} \mathbf{0}_{n_n,n_n} & -\mathbf{A}^T & \mathbf{0}_{n_n,n_d} & \mathbf{K}^T \\ \mathbf{A} & \mathbf{R} & \mathbf{\Phi} & \mathbf{0}_{n_i,n_p} \\ \mathbf{0}_{n_d,n_n} & -\mathbf{\Phi}^T & \mathbf{0}_{n_d,n_d} & \mathbf{0}_{n_d,n_p} \\ -\mathbf{K} & \mathbf{0}_{n_p,n_i} & \mathbf{0}_{n_p,n_d} & \mathbf{0}_{n_p,n_p} \end{bmatrix}}_{\mathbf{G}} \cdot \underbrace{\begin{bmatrix} \mathbf{v}(t) \\ \mathbf{i}(t) \\ \mathbf{v}_d(t) \\ \mathbf{i}_p(t) \end{bmatrix}}_{\mathbf{x}(t)} +$$

$$\underbrace{\begin{bmatrix} \mathbf{0}_{n_n+n_i+n_d,n_p} \\ -\mathbf{I}_{n_p,n_p} \end{bmatrix}}_{\mathbf{B}} \cdot \underbrace{\begin{bmatrix} \mathbf{v}_p(t) \end{bmatrix}}_{\mathbf{u}(t)} \tag{4}$$

where $\mathbf{I}_{n_p,n_p}$ is the identity matrix of dimensions equal to the number of ports. Matrix $\mathbf{\Phi}$ is

$$\mathbf{\Phi} = \begin{bmatrix} \mathbf{0}_{n_c,n_d} \\ \mathbf{I}_{n_d,n_d} \end{bmatrix} \tag{5}$$

In a more compact form, the previous equations can be rewritten as:

$$\mathbf{C}\frac{d\mathbf{x}(t)}{dt} = -\mathbf{G}\mathbf{x}(t) + \mathbf{B}\mathbf{u}(t) \tag{6a}$$

$$\mathbf{i}_p(t) = \mathbf{L}^T\mathbf{x}(t) \tag{6b}$$

where $\mathbf{x}(t) = [\mathbf{v}(t) \quad \mathbf{i}(t) \quad \mathbf{v}_d(t) \quad \mathbf{i}_p(t)]^T$ and $\mathbf{B} = \mathbf{L}$, $\mathbf{B} \in \Re^{n_u \times n_p}$. This is an admittance n_p-port formulation $\mathbf{Y}(s) = \mathbf{L}^T(s\mathbf{C} + \mathbf{G})^{-1}\mathbf{B}$, whereby the only sources are the voltage sources at the n_p-port nodes. If we consider N design parameters $\boldsymbol{g} = (g^{(1)}, ..., g^{(\mathrm{N})})$ in addition to frequency, the equations (6a)-(6b) become

$$\mathbf{C}(\boldsymbol{g})\frac{d\mathbf{x}(t,\boldsymbol{g})}{dt} = -\mathbf{G}(\boldsymbol{g})\mathbf{x}(t,\boldsymbol{g}) + \mathbf{B}(\boldsymbol{g})\mathbf{u}(t) \tag{7a}$$

$$\mathbf{i}_p(t,\boldsymbol{g}) = \mathbf{L}(\boldsymbol{g})^T\mathbf{x}(t,\boldsymbol{g}) \tag{7b}$$

B. Properties of PEEC formulation

When performing transient analysis, stability and passivity must be guaranteed. It is known that, while a passive system is also stable, the reverse is not necessarily true [33], which is crucial when the model is to be utilized in a general-purpose analysis-oriented nonlinear simulator. Passivity refers to the property of systems that cannot generate more energy than they absorb through their electrical ports. When a passive system is terminated on any set of arbitrary passive loads, none of them will cause the system to become unstable [34], [35]. A linear network described by admittance matrix $\mathbf{Y}(s)$ is passive (or positive-real) if [36]:

1) $\mathbf{Y}(s^*) = \mathbf{Y}^*(s)$ for all s, where "$*$" is the complex conjugate operator.
2) $\mathbf{Y}(s)$ is analytic in $\Re e(s) > 0$.
3) $\mathbf{Y}(s)$ is a positive-real matrix, i.e. : $\mathbf{z}^{*T}\left(\mathbf{Y}(s) + \mathbf{Y}^T(s^*)\right)\mathbf{z} \geq 0$; $\forall s : \Re e(s) > 0$ and any arbitrary vector $\mathbf{z}$.

Provided that the matrices $\mathbf{P}^{-1}, \mathbf{L}_p, \mathbf{C}_d, \mathbf{R}$ are symmetric non-negative definite matrices by construction, it is straightforward to prove that the matrices $\mathbf{C}, \mathbf{G}$ satisfy the following properties

$$\mathbf{C} = \mathbf{C}^T \geq 0 \tag{8a}$$

$$\mathbf{G} + \mathbf{G}^T \geq 0 \tag{8b}$$

The properties of the PEEC matrices $\mathbf{B} = \mathbf{L}$, $\mathbf{C} = \mathbf{C}^T \geq 0$, $\mathbf{G} + \mathbf{G}^T \geq 0$ ensure the passivity of the PEEC admittance model $\mathbf{Y}(s) = \mathbf{L}^T(s\mathbf{C} + \mathbf{G})^{-1}\mathbf{B}$ [37] and allow to exploit the passivity-preserving capability of PRIMA [8].

III. Parameterized Model Order Reduction

In this section we describe a parameterized model order reduction algorithm that is able to include, in addition to frequency, N design parameters $\boldsymbol{g} = (g^{(1)}, ..., g^{(\mathrm{N})})$ in the reduced order model, such as the layout features of a circuit (e.g. lengths, widths,...) or the substrate parameters (e.g. thickness, dielectric constant, losses,...). The main objective of the parameterized MOR method is to accurately approximate the original scalable system (having a high complexity) with a reduced

scalable system (having a low complexity) by capturing the behaviour of the original system with respect to frequency and other design parameters. The proposed algorithm guarantees stability and passivity of the parametric reduced model over the entire design space of interest. A flowchart that describes the different steps of the proposed PMOR method is shown in Fig. 2.

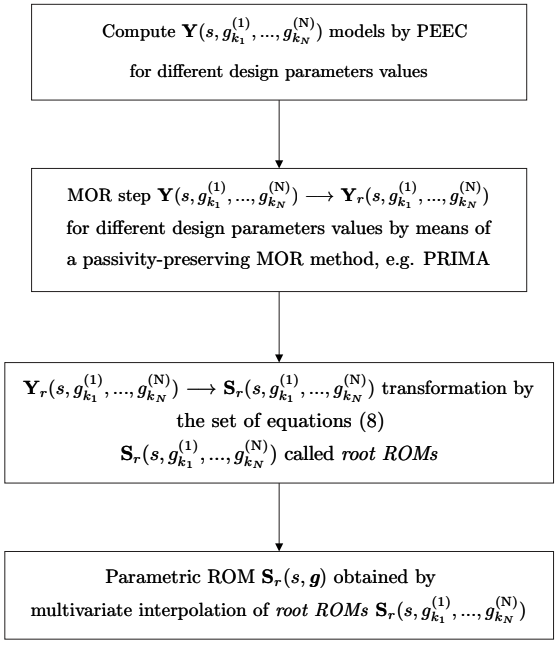

Fig. 2. Flowchart of the proposed PMOR method.

A. Root ROMs

The proposed PMOR technique starts by computing a bunch of stable and passive reduced order models of the PEEC admittance matrix $\mathbf{Y}(s, \boldsymbol{g}) = \mathbf{L}^T(\boldsymbol{g})(s\mathbf{C}(\boldsymbol{g}) + \mathbf{G}(\boldsymbol{g}))^{-1}\mathbf{B}(\boldsymbol{g})$ using the PRIMA algorithm for a set of points in the design space, that we call estimation design space grid. The design space $\mathcal{D}(\boldsymbol{g})$ is considered as the parameter space $\mathcal{P}(s, \boldsymbol{g})$ without frequency. The parameter space $\mathcal{P}(s, \boldsymbol{g})$ contains all parameters $(s, \boldsymbol{g})$. If the parameter space is N-dimensional, the design space is (N-1)-dimensional. Two design space grids are used in the modeling process: an estimation grid and a validation grid. The first grid is utilized to build the *root ROMs*. The second grid is utilized to assess the capability of parametric reduced order models of describing the system under study in a set of points of the design space previously not used for the construction of the *root ROMs*. To clarify the use of these two design space grids, we show in Fig. 3 a possible estimation and validation design space grid in the case of two design parameters $\boldsymbol{g} = (g^{(1)}, g^{(2)})$. A *root ROM* is built for each red (x) point in the design space. The set of *root ROMs* is interpolated, as explained in Sections III-C and III-D, to build a parametric reduced model that is evaluated and compared with original PEEC models related to the blue (o) design space points. We note that these blue (o) points are not used for the generation of the *root ROMs*.

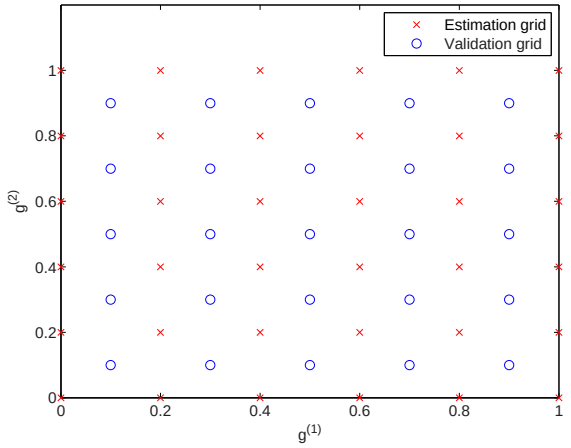

Fig. 3. An example of estimation and validation design space grid.

N-dimensional and scattered design space grids can also be treated by the proposed PMOR technique that does not impose any constraint on the number of design parameters and the distribution of $\boldsymbol{g}$ points in the design space. PRIMA algorithm is used to reduce the PEEC admittance representation $\mathbf{Y}(s, \overline{\boldsymbol{g}})$ for each point $\overline{\boldsymbol{g}}$ in the estimation design space grid. The Krylov subspace and a corresponding projection matrix $\mathbf{V}(\overline{\boldsymbol{g}})$ are built to perform a congruence transformation on the original PEEC matrices $\mathbf{C}(\overline{\boldsymbol{g}}), \mathbf{G}(\overline{\boldsymbol{g}}), \mathbf{B}(\overline{\boldsymbol{g}}), \mathbf{L}(\overline{\boldsymbol{g}})$

$$\begin{aligned}
\mathbf{C_r}(\overline{\boldsymbol{g}}) &= \mathbf{V}(\overline{\boldsymbol{g}})^T\mathbf{C}(\overline{\boldsymbol{g}})\mathbf{V}(\overline{\boldsymbol{g}}) \\
\mathbf{G_r}(\overline{\boldsymbol{g}}) &= \mathbf{V}(\overline{\boldsymbol{g}})^T\mathbf{G}(\overline{\boldsymbol{g}})\mathbf{V}(\overline{\boldsymbol{g}}) \\
\mathbf{B_r}(\overline{\boldsymbol{g}}) &= \mathbf{V}(\overline{\boldsymbol{g}})^T\mathbf{B}(\overline{\boldsymbol{g}}) \\
\mathbf{L_r}(\overline{\boldsymbol{g}}) &= \mathbf{V}(\overline{\boldsymbol{g}})^T\mathbf{L}(\overline{\boldsymbol{g}})
\end{aligned} \tag{9}$$

Since at microwave frequencies, the $\mathbf{Y}$-representation cannot be accurately measured because the required short-circuit tests are difficult to achieve over a broad range of frequencies, the $\mathbf{S}$-representation is used to describe the broadband frequency behavior of microwave systems. Therefore, the reduced models are translated from $\mathbf{Y}$-representation into $\mathbf{S}$-representation preserving stability and passivity by the procedure described in the following Section III-B. In the paper we refer to these initial $\mathbf{S}$-reduced order models as *root ROMs*. This initial step allows the separation of frequency from the other parameters, in other words frequency is treated as a special parameter. The sampling density in the estimation design space grid, which decides the number of *root ROMs*, is important to accurately describe the parameterized behavior of an EM system under study over the entire design space of interest. A technique to choose the number of points in the estimation grid, and consequently the number of *root ROMs*, can be found in [38].

B. Y-S transformation

The definition of $\mathbf{S}$-representation and its relation to the other system representations depend on the reference impedance at each port $Z_{0,i}$, that in practice is often chosen

equal to 50 Ω. Let $\mathbf{Z}_0$ be a real diagonal matrix such that $\mathbf{Z}_0(i,i) = \mathrm{Z}_{0,i}$, the $\mathbf{S}$-representation is related to the $\mathbf{Y}$-representation by

$$\mathbf{S}(s) = \left(\mathbf{I} - \mathbf{Z}_0^{1/2}\mathbf{Y}(s)\mathbf{Z}_0^{1/2}\right)\left(\mathbf{I} + \mathbf{Z}_0^{1/2}\mathbf{Y}(s)\mathbf{Z}_0^{1/2}\right)^{-1} \quad (10)$$

It is possible to obtain a descriptor form $\mathbf{S_r}(s,\overline{\boldsymbol{g}}) = [\widetilde{\mathbf{C}_\mathbf{r}}(\overline{\boldsymbol{g}}), \widetilde{\mathbf{G}_\mathbf{r}}(\overline{\boldsymbol{g}}), \widetilde{\mathbf{B}_\mathbf{r}}(\overline{\boldsymbol{g}}), \widetilde{\mathbf{L}_\mathbf{r}}(\overline{\boldsymbol{g}}), \widetilde{\mathbf{D}_\mathbf{r}}(\overline{\boldsymbol{g}})]$ from a descriptor form of the reduced order model $\mathbf{Y_r}(s,\overline{\boldsymbol{g}}) = [\mathbf{C_r}(\overline{\boldsymbol{g}}), \mathbf{G_r}(\overline{\boldsymbol{g}}), \mathbf{B_r}(\overline{\boldsymbol{g}}), \mathbf{L_r}(\overline{\boldsymbol{g}})]$ obtained by means of PRIMA, using the following equations [39]

$$\begin{aligned}
\widetilde{\mathbf{C}_\mathbf{r}}(\overline{\boldsymbol{g}}) &= \mathbf{C_r}(\overline{\boldsymbol{g}}) \\
\widetilde{\mathbf{G}_\mathbf{r}}(\overline{\boldsymbol{g}}) &= \mathbf{G_r}(\overline{\boldsymbol{g}}) + \mathbf{B_r}(\overline{\boldsymbol{g}})\mathbf{Z}_0\mathbf{L_r}(\overline{\boldsymbol{g}})^T \\
\widetilde{\mathbf{B}_\mathbf{r}}(\overline{\boldsymbol{g}}) &= \sqrt{2}\mathbf{B_r}(\overline{\boldsymbol{g}})\mathbf{Z}_0^{1/2} \\
\widetilde{\mathbf{L}_\mathbf{r}}(\overline{\boldsymbol{g}}) &= -\widetilde{\mathbf{B}_\mathbf{r}}(\overline{\boldsymbol{g}}) \\
\widetilde{\mathbf{D}_\mathbf{r}}(\overline{\boldsymbol{g}}) &= \mathbf{I}
\end{aligned} \quad (11)$$

We note that the transfer function $\mathbf{Y}(s)$ is positive-real if and only if $\mathbf{S}(s)$ is bounded-real [36], i.e.:

1) $\mathbf{S}(s^*) = \mathbf{S}^*(s)$ for all s, where "$*$" is the complex conjugate operator.
2) $\mathbf{S}(s)$ is analytic in $\Re e(s) > 0$.
3) $\mathbf{I} - \mathbf{S}^T(s^*)\mathbf{S}(s) \geq 0$; $\forall s : \Re e(s) > 0$.

The bounded-realness property represents the passivity property for systems described by scattering parameters. Once a passive and stable $\mathbf{Y}$-reduced model is obtained by means of PRIMA, a transformation from $\mathbf{Y}$ into $\mathbf{S}$ is performed using the set of equations (11), which results in a reduced $\mathbf{S}$-representation that is still stable and passive. If Krylov-subspace-based MOR algorithms (e.g. PRIMA [8], Laguerre-SVD [24]) are used to build the *root ROMs*, no error bound is provided for them. Hence, the selection of the reduced order for each *root ROM* is performed by a bottom-up approach, it is increased as long as the maximum absolute error of each *root ROM* ($\mathbf{S}$-representation) is larger than -60 dB over the frequency range of interest that is suitably sampled.

C. 2-D PMOR

First, we discuss the representation of a bivariate reduced model and afterwards the generalization to more dimensions. Once the *root ROMs* are available, the next step is to find a bivariate reduced model $\mathbf{S}_r(s,g)$ that: 1) is able to accurately describe the system under study in design space points previously not used for the generation of the *root ROMs* (the validation design space grid is used to test this modeling capability), 2) is able to preserve stability and passivity over the entire design space. The bivariate reduced model we adopt can be written as

$$\mathbf{S}_r(s,g) = \sum_{k=1}^{K_1} \mathbf{S}_r(s,g_k)\ell_k(g) \quad (12)$$

where K_1 is the number of the *root ROMs*, and the interpolation kernels $\ell_k(g)$ are scalar functions satisfying the following constraints

$$0 \leq \ell_k(g) \leq 1, \quad (13)$$

$$\ell_k(g_i) = \delta_{k,i}, \quad (14)$$

$$\sum_{k=1}^{K_1} \ell_k(g) = 1. \quad (15)$$

A suitable choice is to select the set $\ell_k(g)$ as in piecewise linear interpolation

$$\frac{g - g_{k-1}}{g_k - g_{k-1}},\ g \in [g_{k-1}, g_k]\,,\ k = 2, ..., K_1, \quad (16a)$$

$$\frac{g_{k+1} - g}{g_{k+1} - g_k},\ g \in [g_k, g_{k+1}]\,,\ k = 1, ..., K_1 - 1, \quad (16b)$$

$$0 \qquad\qquad ,\ \text{otherwise.} \quad (16c)$$

The reduced model in (12) is a linear combination of stable and passive univariate reduced models by means of a class of positive interpolation kernels [21]. Stability is automatically preserved in (12), since it is a weighted sum of stable rational models of s. The proof of the passivity-preserving property of the proposed PMOR scheme over the entire design space is given in Section III-E.

D. (N+1)-D PMOR

The bivariate formulation (12) can easily be generalized to the multivariate case by using multivariate interpolation methods. Multivariate interpolation can be realized by means of tensor product [40] or tessellation [41] methods. Tensor product multivariate interpolation methods require that the data points are distributed on a fully filled, but not necessarily equidistant, rectangular grid, while tessellation-based multivariate interpolation methods can handle scattered or irregularly distributed data points. For the sake of clarity, we show in Fig. 4 how a parametric reduced order model is built in a 2-D design space by means of interpolation of *root ROMs*.

1) Tensor product multivariate interpolation: The parametric reduced model can be written as

$$\begin{aligned}
&\mathbf{S}_r(s,\boldsymbol{g}) = \\
&= \sum_{k_1=1}^{K_1} \cdots \sum_{k_N=1}^{K_N} \mathbf{S}_r(s, g_{k_1}^{(1)}, ..., g_{k_N}^{(\mathrm{N})})\ell_{k_1}(g^{(1)}) \cdots \ell_{k_N}(g^{(\mathrm{N})})
\end{aligned} \quad (17)$$

where $\ell_{k_i}(g^{(i)})$, $i = 1, ..., \mathrm{N}$ satisfy all constraints (13)-(15). A suitable choice is to select each set $\ell_{k_i}(g^{(i)})$ as in piecewise linear interpolation, which yields to an interpolation scheme in (17) called piecewise multilinear. This method can be also seen as a recursive implementation of 1-D piecewise linear interpolation. We remark that the interpolation process is local, because the parametric reduced model $\mathbf{S}_r(s,\boldsymbol{g})$ at a specific point $\widehat{\boldsymbol{g}}$ in the design space $\mathcal{D}(\boldsymbol{g})$ only depends on the *root ROMs* at the vertices of the hypercube that contains the point $\widehat{\boldsymbol{g}}$. An hypercube in $\mathbb{R}^\mathrm{N}$ has 2^N vertices, 2^N increases exponentially with the number of dimensions, but

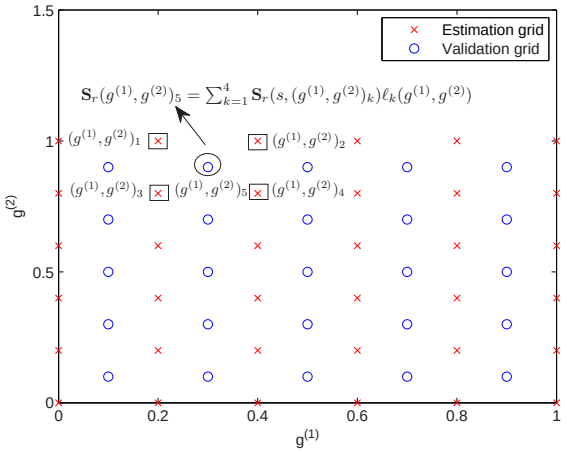

Fig. 4. Example of a parametric reduced model in a 2-D design space obtained by means of interpolation of *root ROMs*.

it still remains much smaller than the number of data points $K_1 \cdot K_2 \cdot ... \cdot K_{\mathrm{N}}$ in the fully filled design space grid. This multivariate interpolation method belongs to the general class of positive interpolation schemes [21].

2) Multivariate simplicial interpolation: Before performing the multivariate simplicial interpolation process, the design space is divided into cells using simplices [41], resulting in a geometric structure that connects the points of the estimation design space grid. In 2-D this process is called triangulation, while in higher dimensions it is called tessellation. A simplex, or N-simplex, is the N-D analogue of a triangle in 2-D and a tetrahedron in 3-D. Fig. 5 shows a possible triangulation of a 2-D design space starting from a regular and a scattered estimation grid, respectively.

A simplex in N dimensions has N+1 vertices. For each data distribution many tessellations can be constructed. The minimal requirement is that the simplices do not overlap, and that there are no holes. Kuhn tessellation [42] can be used for a fully filled design space grid, such technique splits every hypercube in $\mathbb{R}^{\mathrm{N}}$ into N! simplices. Delaunay tessellation [41] can be used for an irregular design space grid, such technique is a space-filling aggregate of simplices and can be performed using standard algorithms [43]. We indicate a simplex region of the design space as $\Omega_i,\ i = 1, ..., \mathrm{P}$ and the corresponding N+1 vertices as $\boldsymbol{g}_k^{\Omega_i},\ k = 1, ..., \mathrm{N}{+}1$. Once the tessellation of the design space is accomplished, a tessellation-based linear interpolation (TLI) is used to build a parametric reduced order model. TLI performs a linear interpolation inside a simplex using barycentric coordinates [44] as interpolation kernels and it is therefore a local method. If the N-dimensional volume of the simplex does not vanish, i.e. it is non-degenerate, any point enclosed by a simplex can be expressed uniquely as a linear combination of the N+1 simplex vertices. A parametric reduced model can be written as:

$$\mathbf{S}_r(s,\boldsymbol{g}) = \sum_{k=1}^{N+1} \mathbf{S}_r(s,\boldsymbol{g}_k^{\Omega_i})\ell_k^{\Omega_i}(\boldsymbol{g}) \tag{18}$$

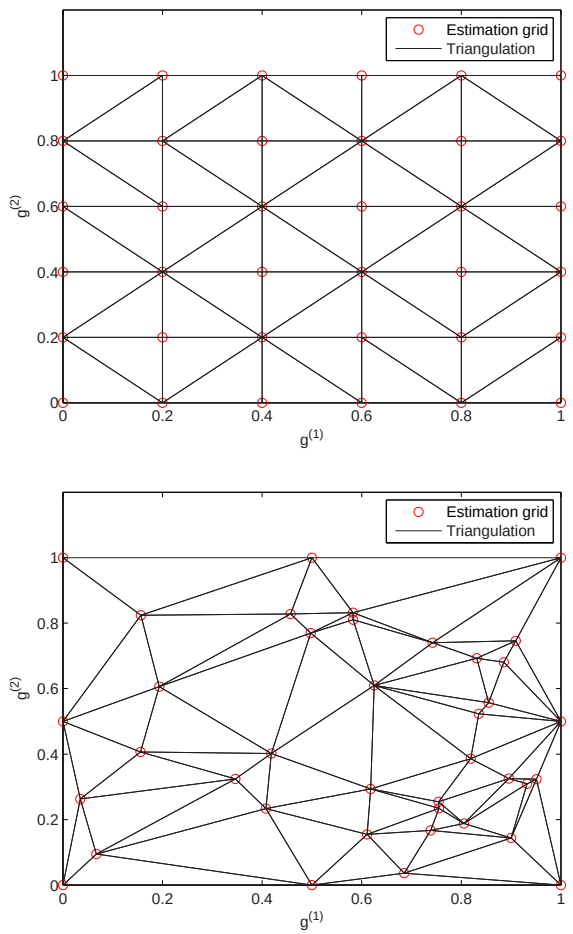

Fig. 5. Triagulation of a 2-D design space starting from a regular (top) and a scattered (bottom) estimation grid.

where Ω_i is the simplex the contains the point $\boldsymbol{g}$ and the barycentric coordinates $\ell_k^{\Omega_i}(\boldsymbol{g})$ satisfy the following properties

$$0 \leq \ell_k^{\Omega_i}(\boldsymbol{g}) \leq 1 \tag{19}$$

$$\ell_k^{\Omega_i}(\boldsymbol{g}_i^{\Omega_i}) = \delta_{k,i} \tag{20}$$

$$\sum_{k=1}^{N+1} \ell_k^{\Omega_i}(\boldsymbol{g}) = 1 \tag{21}$$

We remark that the interpolation process is local, because the parametric reduced model $\mathbf{S}_r(s,\boldsymbol{g})$ at a specific point $\widehat{\boldsymbol{g}}$ in the design space $\mathcal{D}(\boldsymbol{g})$ only depends on the N+1 *root ROMs* at the vertices of the simplex that contains the point $\widehat{\boldsymbol{g}}$. The TLI method belongs to the general class of positive interpolation schemes [21]. Stability is automatically preserved in (17)-(18), since they are weighted sums of stable rational models of s. The proof of the passivity-preserving property of the proposed PMOR schemes over the entire design space is given in Section III-E. We note that the interpolation kernels we propose only depend on the design space grid points and their computation does not require the solution of a linear system to impose an interpolation constraint. The proposed PMOR technique is able to deal with fully filled and scattered design

space grids. It is general and any interpolation scheme that leads to a parametric reduced model composed of a weighted sum of *root ROMs* with weights satisfying (13)-(15) can be used. The error distribution of parametric reduced models obtained by the proposed PMOR technique is related to the utilized interpolation scheme and the error of the *root ROMs*.

E. Passivity-Preserving Interpolation

In this section we prove that the proposed PMOR method preserves passivity over the entire design space. Concerning the *root ROMs*, we have already proven in Section III-B that all three bounded-realness conditions are satisfied. Condition 1) is preserved in (12) and the proposed multivariate extensions (17)-(18), since they are weighted sums with real nonnegative weights of systems respecting this first condition. Condition 2) is preserved in (12), (17), (18), since they are weighted sums of stable rational reduced models of s. Condition 3) is equivalent to $\|\mathbf{S}(s)\|_\infty \leq 1$ ($\mathbf{H}_\infty$ norm) [45], i.e., the largest singular value of $\mathbf{S}(s)$ does not exceed one in the right-half s-plane. Using this equivalent condition, in the bivariate case we can write

$$\|\mathbf{S}_r(s,g)\|_\infty \leq \sum_{k=1}^{K_1} \|\mathbf{S}_r(s,g_k)\|_\infty \; \ell_k(g) \leq \sum_{k=1}^{K_1} \ell_k(g) = 1 \tag{22}$$

Similar results are obtained for the proposed multivariate cases (17)-(18), so condition 3) is satisfied by construction using our PMOR method. We have demonstrated that all three bounded-realness conditions are preserved in the novel PMOR algorithm, using the sufficient conditions (13)-(15) related to the interpolation kernels.

F. Passivity assessment considerations

The properties of the PEEC matrices, the PRIMA algorithm, the $\mathbf{Y}-\mathbf{S}$ transformation procedure and the proposed multivariate interpolation schemes ensure overall stability and passivity for the parametric reduced order model $\mathbf{S}_r(s,\boldsymbol{g})$ by construction. Although no passivity check is required for $\mathbf{S}_r(s,\boldsymbol{g})$, the authors describe in this section a passivity test for the sake of completeness. Let us assume that $\mathbf{S}_r(s,\boldsymbol{g})$ is obtained and one wants to carry a passivity test out for a specific point $\widehat{\boldsymbol{g}}$ in the design space. If the descriptor matrix $\widetilde{\mathbf{C}_\mathbf{r}}(\widehat{\boldsymbol{g}})$ of $\mathbf{S}_r(s,\widehat{\boldsymbol{g}})$ is singular, the procedure described in [46] is used to convert the descriptor system into a standard state-space model

$$\frac{d\boldsymbol{x}(t)}{dt} = \mathcal{A}\boldsymbol{x}(t) + \mathcal{B}\boldsymbol{u}(t) \tag{23a}$$

$$\boldsymbol{y}(t) = \mathcal{C}\boldsymbol{x}(t) + \mathcal{D}\boldsymbol{u}(t) \tag{23b}$$

otherwise the standard state-space model can be obtained by

$$\begin{aligned} \mathcal{A} &= -\widetilde{\mathbf{C}_\mathbf{r}}(\widehat{\boldsymbol{g}})^{-1}\widetilde{\mathbf{G}_\mathbf{r}}(\widehat{\boldsymbol{g}}) \\ \mathcal{B} &= \widetilde{\mathbf{C}_\mathbf{r}}(\widehat{\boldsymbol{g}})^{-1}\widetilde{\mathbf{B}_\mathbf{r}}(\widehat{\boldsymbol{g}}) \\ \mathcal{C} &= \widetilde{\mathbf{B}_\mathbf{r}}(\widehat{\boldsymbol{g}})^T \\ \mathcal{D} &= \widetilde{\mathbf{D}_\mathbf{r}}(\widehat{\boldsymbol{g}}) \end{aligned} \tag{24}$$

Once $\mathbf{S}_r(s,\widehat{\boldsymbol{g}})$ is transformed into a standard state-space form, its passivity can be verified by computing the eigenvalues of an associated Hamiltonian matrix [45]

$$\tilde{\mathcal{H}} = \begin{bmatrix} \mathcal{A} - \mathcal{B}\mathcal{R}^{-1}\mathcal{D}^T\mathcal{C} & -\mathcal{B}\mathcal{R}^{-1}\mathcal{B}^T \\ \mathcal{C}^T\mathcal{Q}^{-1}\mathcal{C} & -\mathcal{A}^T + \mathcal{C}^T\mathcal{D}\mathcal{R}^{-1}\mathcal{B}^T \end{bmatrix} \tag{25}$$

with $\mathcal{R} = \mathcal{D}^T\mathcal{D} - \mathbf{I}$ and $\mathcal{Q} = \mathcal{D}\mathcal{D}^T - \mathbf{I}$. This passivity test can only be applied if $\mathcal{D}^T\mathcal{D} - \mathbf{I}$ is not singular. If such singularity exists, the modified Hamiltonian-based passivity check proposed in [47] should be used.

IV. Numerical results

A. 2-D example: Microstrip line

In the first example a microstrip line with a dispersive DriClad dielectric $\varepsilon_r = 4.1$ and a length $\ell = 2$ cm has been modeled. Its cross section is shown in Fig. 6. The dielectric and conductor thickness values are $h = 600$ μm and $t = 100$ μm, respectively. A bivariate reduced order model is built as a function of frequency and the width of the strip W. Their corresponding ranges are shown in Table I.

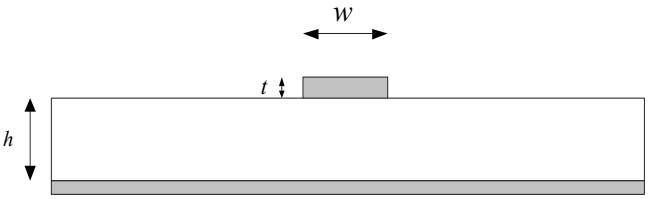

Fig. 6. Cross section of the microstrip.

TABLE I
PARAMETERS OF THE MICROSTRIP STRUCTURE.

Parameter	Min	Max
Frequency (freq)	1 kHz	4 GHz
Width (W)	50 μm	250 μm

The PEEC method is used to compute the $\mathbf{C},\mathbf{G},\mathbf{B},\mathbf{L}$ matrices in (6a)-(6b) for 30 values of the width. The order of all original PEEC models is equal to $n_u = 2532$. Then, we have built reduced models for 12 values of the width by means of PRIMA, each with a reduced order $q = 20$. A $\mathbf{Y}-\mathbf{S}$ transformation has been performed choosing $\mathrm{Z}_{0,1} = \mathrm{Z}_{0,2} = 50\ \Omega$, which results in a set of 12 *root ROMs*. A bivariate reduced model $\mathbf{S}_r(s,W)$ is obtained by piecewise linear interpolation of the *root ROMs*. The passivity of the parametric reduced model has been checked by the procedure described in Section III-F on a dense sweep over the design space and the theoretical claim of overall passivity has been confirmed. Fig. 7 shows the magnitude of the parametric reduced model of $\mathbf{S}_{11}(s,W)$. Fig. 8 shows the magnitude of the parametric reduced models of $\mathbf{S}_{11}(s,W)$ and $\mathbf{S}_{21}(s,W)$ for the width values $W = \{55, 150, 245\}$ μm. These specific width values have not been used in the *root ROMs* generation process, nevertheless an excellent agreement between model and data can be observed. Fig. 9 shows the absolute error distribution

for $\mathbf{S}_{11}(s,W)$ and $\mathbf{S}_{21}(s,W)$ over a dense reference grid composed of 200×30 $(freq, W)$ samples. The maximum absolute error of the bivariate reduced model of the $\mathbf{S}$ matrix over the reference grid is bounded by -60.57 dB. As clearly seen, the parametric reduced model captures very accurately the behavior of the system, while guaranteeing stability and passivity properties over the entire design space.

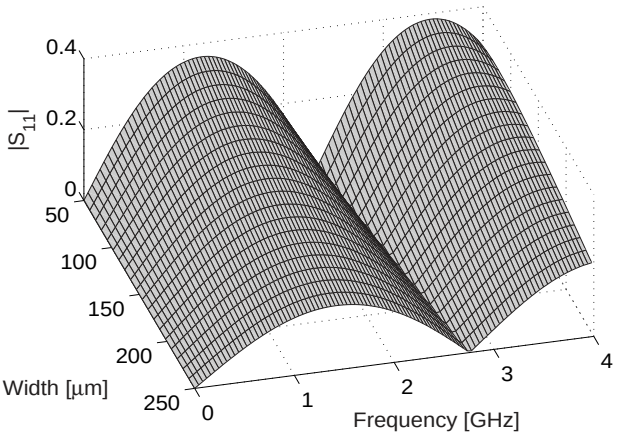

Fig. 7. Magnitude of the bivariate reduced model of $\mathbf{S}_{11}(s,W)$.

B. 3-D example: Multiconductor system with variable separation

This example reproduces the geometry of a multiconductor system composed by six conductors with a length $\ell = 2$ cm, a width $W = 1$ mm and a thickness $t = 0.2$ mm. The cross section is shown in Fig. 10 and depends on the two variables S_x and S_y that represent the horizontal and vertical spacing between the conductors. A trivariate reduced order model is built as a function of frequency and the horizontal and vertical spacing. Their corresponding ranges are shown in Table II.

TABLE II
PARAMETERS OF THE MULTICONDUCTOR SYSTEM.

Parameter	Min	Max
Frequency (freq)	1 kHz	15 GHz
Horizontal spacing (S_x)	2 mm	3 mm
Vertical spacing (S_y)	1 mm	2 mm

The PEEC method is used to compute the $\mathbf{C}, \mathbf{G}, \mathbf{B}, \mathbf{L}$ matrices in (6a)-(6b) for 15 values of S_x and 15 values of S_y. The order of all original PEEC models is equal to $n_u = 702$. Then, we have built reduced models for 5 values of S_x and 8 values of S_y by means of PRIMA, each with a reduced order $q = 54$. A $\mathbf{Y} - \mathbf{S}$ transformation has been performed choosing $\mathrm{Z}_{0,i} = 50\ \Omega,\ i = 1, ..., 6$, which results in a set of 40 *root ROMs*. The ports of the system are six and are defined between a conductor and the corresponding one above. A trivariate reduced model $\mathbf{S}_r(s, S_x, S_y)$ is obtained by piecewise multilinear and multivariate simplicial interpolation of the *root ROMs*. The passivity of the parametric reduced

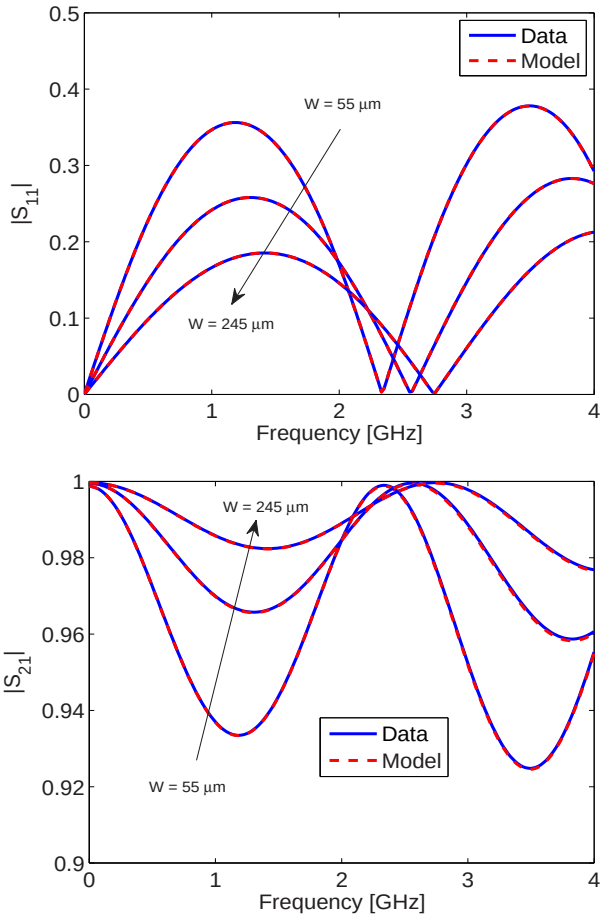

Fig. 8. Magnitude of the bivariate reduced models of $\mathbf{S}_{11}(s,W)$ and $\mathbf{S}_{21}(s,W)$ ($W = \{55, 150, 245\}$ μm).

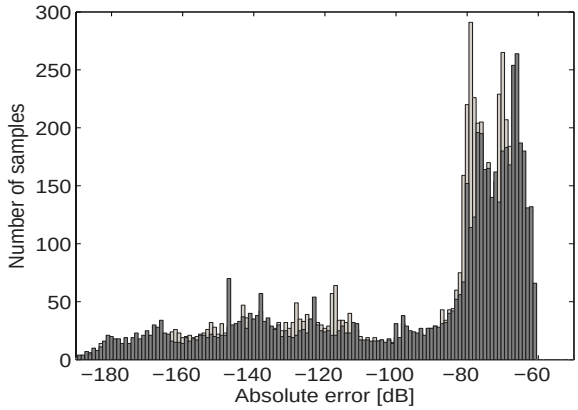

Fig. 9. Histogram : error distributions of the bivariate reduced models of $\mathbf{S}_{11}(s,W)$ (light grey) and $\mathbf{S}_{21}(s,W)$ (dark grey) over 6000 validation samples.

models has been checked by the procedure described in Section III-F on a dense sweep over the design space and the theoretical claim of overall passivity has been confirmed. Figs. 11-12 show the magnitude of the parametric reduced model of the forward crosstalk term $\mathbf{S}_{16}(s, S_x, S_y)$ (input

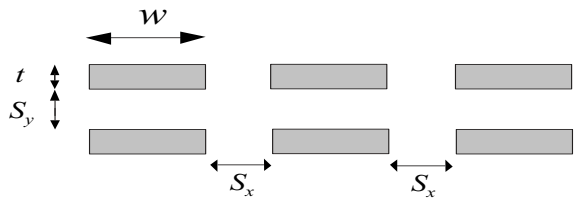

Fig. 10. Cross section of the multiconductor system.

port of the first couple of conductors on the left and output port of the first couple of conductors on the right) obtained by piecewise multilinear interpolation for the vertical spacing values $S_y = \{1, 2\}$ mm. Similar results are obtained using the multivariate simplicial interpolation scheme. Fig. 13 shows the magnitude of the parametric reduced model of $\mathbf{S}_{11}(s, S_x, S_y)$ obtained by multivariate simplicial interpolation for the horizontal spacing value $S_x = 2.5$ mm and the vertical spacing values $S_y = \{1.07, 1.5, 1.93\}$ mm. These specific spacing values have not been used in the *root ROMs* generation process. Fig. 14 shows the magnitude of the parametric reduced model of $\mathbf{S}_{16}(s, S_x, S_y)$ obtained by multivariate simplicial interpolation for the horizontal spacing values $S_x = \{2.07, 2.5, 2.93\}$ mm and the vertical spacing value $S_y = 1.5$ mm. These specific spacing values have not been used in the *root ROMs* generation process. Figs. 15-16 show the absolute error distribution for $\mathbf{S}_{11}(s, S_x, S_y)$ and $\mathbf{S}_{16}(s, S_x, S_y)$ over a reference grid composed of $300 \times 15 \times 15$ $(freq, S_x, S_y)$ samples. The maximum absolute error of the trivariate reduced model of the $\mathbf{S}$ matrix over the reference grid is bounded by -60.5 dB and -61.44 dB, respectively for the piecewise multilinear and multivariate simplicial interpolation scheme. As in the previous example, the parametric reduced order model describes the behavior of the system under study very accurately, while guaranteeing overall stability and passivity.

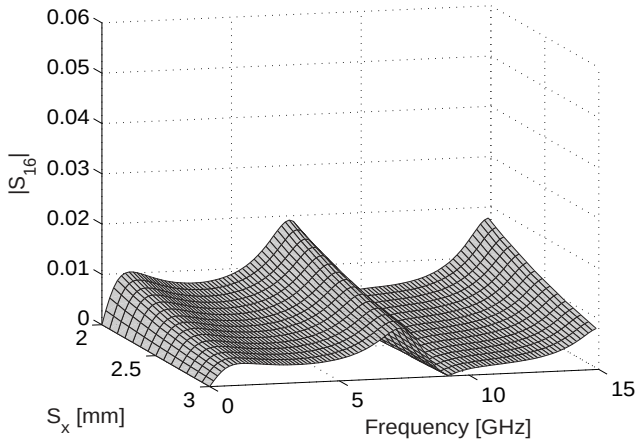

Fig. 11. Magnitude of the trivariate reduced model of $\mathbf{S}_{16}(s, S_x, S_y)$ (piecewise multilinear interpolation, $S_y = 1$ mm).

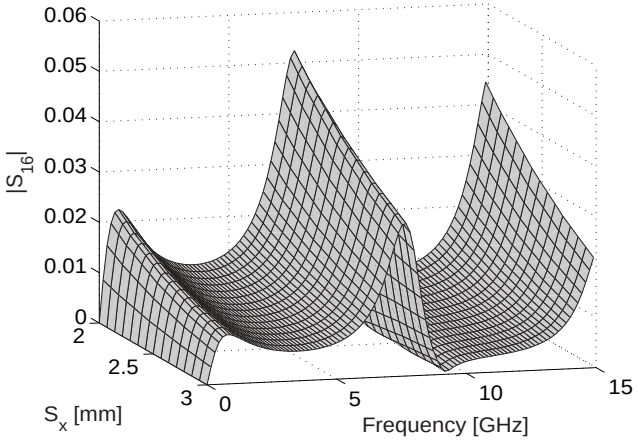

Fig. 12. Magnitude of the trivariate reduced model of $\mathbf{S}_{16}(s, S_x, S_y)$ (piecewise multilinear interpolation, $S_y = 2$ mm).

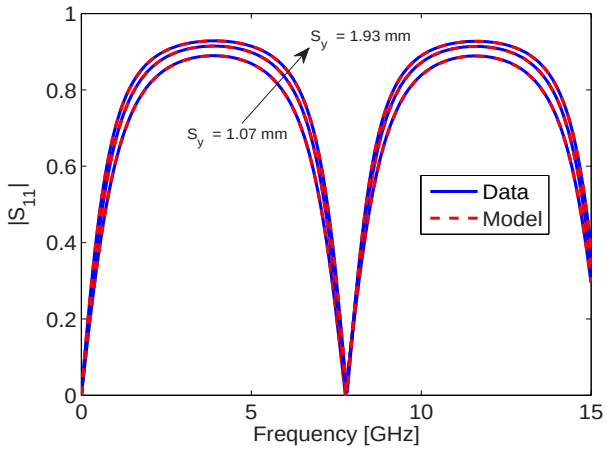

Fig. 13. Magnitude of the trivariate reduced model of $\mathbf{S}_{11}(s, S_x, S_y)$ (multivariate simplicial interpolation, $S_x = 2.5$ mm, $S_y = \{1.07, 1.5, 1.93\}$ mm).

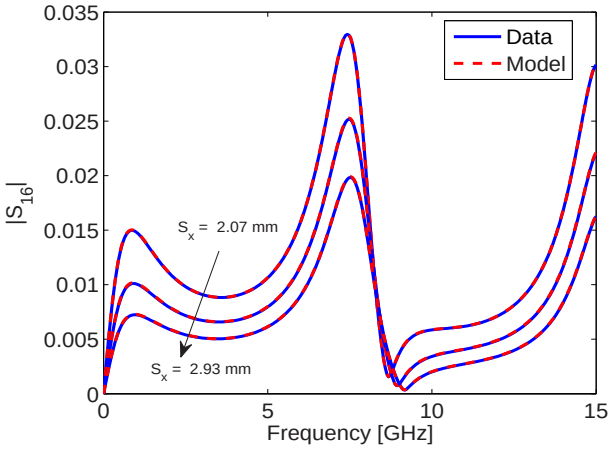

Fig. 14. Magnitude of the trivariate reduced model of $\mathbf{S}_{16}(s, S_x, S_y)$ (multivariate simplicial interpolation, $S_x = \{2.07, 2.5, 2.93\}$ mm, $S_y = 1.5$ mm).

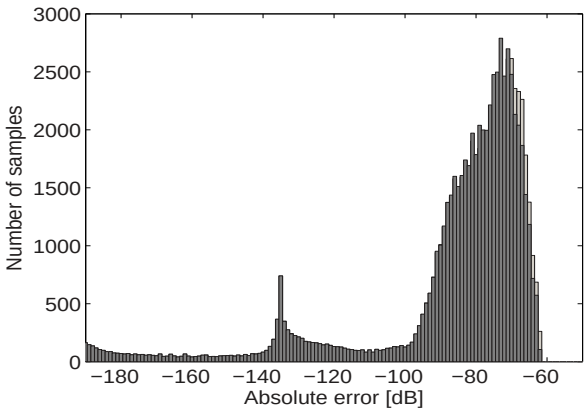

Fig. 15. Histogram : error distributions of the trivariate reduced models of $\mathbf{S}_{11}(s, S_x, S_y)$ (piecewise multilinear interpolation, light grey) and $\mathbf{S}_{11}(s, S_x, S_y)$ (multivariate simplicial interpolation, dark grey) over 67500 validation samples.

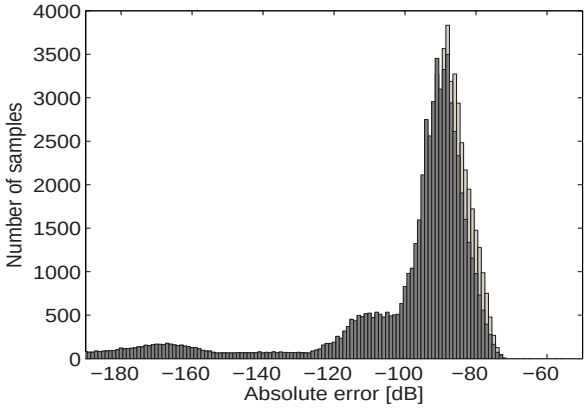

Fig. 16. Histogram : error distributions of the trivariate reduced models of $\mathbf{S}_{16}(s, S_x, S_y)$ (piecewise multilinear interpolation, light grey) and $\mathbf{S}_{16}(s, S_x, S_y)$ (multivariate simplicial interpolation, dark grey) over 67500 validation samples.

V. Conclusions

We have presented a new parameterized model order reduction technique applicable to PEEC analysis. The overall stability and passivity of the parametric reduced order model is guaranteed by an efficient and reliable combination of traditional passivity-preserving MOR methods and interpolation schemes based on a class of positive interpolation operators. Numerical examples have validated the proposed approach on practical application cases, showing that it is able to build very accurate parametric reduced models, while guaranteeing stability and passivity over the entire design space of interest.

References

[1] R. F. Harrington, *Field Computation by Moment Methods*. New York: Macmillan, 1968.

[2] A. E. Ruehli, "Equivalent circuit models for three dimensional multiconductor systems," *IEEE Trans. Microw. Theory Tech.*, vol. 22, no. 3, pp. 216–221, Mar. 1974.

[3] J. M. Jin, *The Finite Element Method in Electromagnetics*, 2nd ed. John Wiley and Sons, New York, 2002.

[4] L. T. Pillage and R. A. Rohrer, "Asymptotic waveform evaluation for timing analysis," *IEEE Trans. Comput.-Aided Design Integr. Circuits Syst.*, vol. 9, no. 4, pp. 352–366, Apr. 1990.

[5] K. Gallivan, E. Grimme, P. Van Dooren, "Asymptotic waveform evaluation via a Lanczos method," *Applied Math.*, vol. 7, no. 5, pp. 75–80, Sep. 1994.

[6] P. Feldmann and R. W. Freund, "Efficient linear circuit analysis by Padé approximation via the Lanczos process," *IEEE Trans. Comput.-Aided Design Integr. Circuits Syst.*, vol. 14, no. 5, pp. 639–649, May 1995.

[7] K. Gallivan, E. Grimme, P. Van Dooren, "A rational Lanczos algorithm for model reduction," *Numerical Algorithms*, vol. 12, pp. 33–63, 1996.

[8] A. Odabasioglu, M. Celik, and L. T. Pileggi, "PRIMA: passive reduced-order interconnect macromodeling algorithm," *IEEE Trans. Comput.-Aided Design Integr. Circuits Syst.*, vol. 17, no. 8, pp. 645–654, Aug. 1998.

[9] A. Dounavis, E. Gad, R. Achar, M. S. Nakhla, "Passive model reduction of multiport distributed interconnects," *IEEE Trans. Microw. Theory Tech.*, vol. 48, no. 12, pp. 2325–2334, Dec. 2000.

[10] R. Achar, P. K. Gunupudi, M. Nakhla, E. Chiprout, "Passive interconnect reduction algorithm for distributed/measured networks," *IEEE Trans. Circuits Syst. II*, vol. 47, no. 4, pp. 287–301, Apr. 2000.

[11] R. Achar, M. Nakhla, "Simulation of high-speed interconnects," *Proc. IEEE*, vol. 89, no. 5, pp. 693–728, May 2001.

[12] A. E. Ruehli and A. C. Cangellaris, "Progress in the methodologies for the electrical modeling of interconnects and electronic packages," *Proc. IEEE*, vol. 89, no. 5, pp. 740–771, May 2001.

[13] R. D. Slone, W. T. Smith, Z. Bai, "Using partial element equivalent circuit full wave analysis and Padé via Lanczos to numerically simulate EMC problems," in *Proc. IEEE Int. Symp. Electromagn. Compat.*, Austin, Tx, Aug. 1997, pp. 608–613.

[14] Y. Liu, L. T. Pileggi, and A. J. Strojwas, "Model order-reduction of RC(L) interconnect including variational analysis," in *Proc. IEEE/AMC Des. Autom. Conf.*, 1999, pp. 201–206.

[15] P. Heydari and M. Pedram, "Model reduction of variable-geometry interconnects using variational spectrally-weighted balanced truncation," in *Proc. IEEE/ACM Int. Conf. Comput.-Aided Des.*, Nov. 4–8, 2001, pp. 586–591.

[16] J. R. Phillips, "Variational interconnect analysis via PMTBR," in *Proc. IEEE/ACM Int. Conf. Comput.-Aided Des.*, Nov. 7–11, 2004, pp. 872–879.

[17] P. K. Gunupudi, R. Khazaka, M. S. Nakhla, T. Smy, and D. Celo, "Passive parameterized time-domain macromodels for high-speed transmission-line networks," *IEEE Trans. Microw. Theory Tech.*, vol. 51, no. 12, pp. 2347–2354, Dec. 2003.

[18] L. Daniel, O. C. Siong, L. S. Chay, K. H. Lee, and J. White, "A multiparameter moment-matching model-reduction approach for generating geometrically parameterized interconnect performance models," *IEEE Trans. Comput.-Aided Design Integr. Circuits Syst.*, vol. 23, no. 5, pp. 678–693, May 2004.

[19] X. Li, P. Li, and L. T. Pileggi, "Parameterized interconnect order reduction with explicit-and-implicit multi-parameter moment matching for inter/intra-die variations," in *Proc. IEEE/ACM Int. Conf. Comput.-Aided Des.*, Nov. 6–10, 2005, pp. 806–812.

[20] Y.-T. Li, Z. Bai, Y. Su, and X. Zeng, "Model order reduction of parameterized interconnect networks via a two-directional arnoldi process," *IEEE Trans. Comput.-Aided Design Integr. Circuits Syst.*, vol. 27, no. 9, pp. 1571–1582, Sep. 2008.

[21] G. Allasia, "Simultaneous interpolation and approximation by a class of multivariate positive operators," *Numerical Algorithms*, vol. 34, no. 2, pp. 147–158, Dec. 2003.

[22] F. Ferranti, L. Knockaert, and T. Dhaene, "Parameterized S-parameter based macromodeling with guaranteed passivity," *IEEE Microw. Wireless Compon. Lett.*, vol. 19, no. 10, pp. 608–610, Oct. 2009.

[23] ——, "Passivity-preserving interpolation-based parameterized macromodeling of scattered S-data," *IEEE Microw. Wireless Compon. Lett.*, vol. 20, no. 3, pp. 133–135, Mar. 2010.

[24] L. Knockaert and D. De Zutter, "Laguerre-SVD reduced-order modeling," *IEEE Trans. Microw. Theory Tech.*, vol. 48, no. 9, pp. 1469–1475, Sep. 2000.

[25] J. R. Phillips, L. Daniel, and L. M. Silveira, "Guaranteed passive balancing transformations for model order reduction," *IEEE Trans. Comput.-Aided Design Integr. Circuits Syst.*, vol. 22, no. 8, pp. 1027–1041, Aug. 2003.

[26] P. J. Restle, A. Ruehli, S. G. Walker, G. Papadopoulos, "Full-Wave PEEC Time-Domain for the Modeling of On-Chip Interconnects," *IEEE Transactions on Computer-Aided Design*, vol. 20, no. 7, pp. 877–887, Jul. 2001.

[27] G. Wollenberg, A. Görisch, "Analysis of 3-D interconnect structures with PEEC using SPICE," *IEEE Trans. Electromagn. Compat.*, vol. 41, no. 2, pp. 412–417, Nov. 1999.
[28] G. Antonini, A. Orlandi, "A wavelet based time domain solution for PEEC circuits," *IEEE Trans. Circuits Syst.*, vol. 47, no. 11, pp. 1634–1639, Nov. 2000.
[29] J. Cullum, A. Ruehli, T. Zhang, "A method for reduced-order modeling and simulation of large interconnect circuits and its application to PEEC models with retardation," *IEEE Trans. Circuits Syst. II*, vol. 47, no. 4, pp. 261–373, Apr. 2000.
[30] A. E. Ruehli, G. Antonini, J. Esch, J. Ekman, A. Mayo and A. Orlandi, "Non-orthogonal PEEC formulation for time and frequency domain EM and circuit modeling," *IEEE Trans. Electromagn. Compat.*, vol. 45, no. 2, pp. 167–176, May 2003.
[31] A. E. Ruehli, H. Heeb, "Circuit models for three-dimensional geometries including dielectrics," *IEEE Trans. Microw. Theory Tech.*, vol. 40, no. 7, pp. 1507–1516, July 1992.
[32] C. Ho, A. Ruehli, P. Brennan, "The modified nodal approach to network analysis," *IEEE Trans. Circuits Syst.*, vol. 22, no. 6, pp. 504–509, Jun. 1975.
[33] R. Rohrer, H. Nosrati, "Passivity considerations in stability studies of numerical integration algorithms," *IEEE Trans. Circuits Syst.*, no. 9, pp. 857–866, Sep. 1981.
[34] L. Weinberg, *Network Analysis and Synthesis*. New York: McGraw-Hill Book Company, 1962.
[35] E. A. Guillemin, *Synthesis of Passive Networks*. John Wiley and Sons, New York, 1957.
[36] B. D. Anderson, S. Vongpanitlerd, *Network Analysis and Synthesis*. Englewood Cliffs, NJ, 1973.
[37] R. W. Freund, "Krylov-subspace methods for reduced-order modeling in circuit simulation," *J. Comput. Appl. Math.*, vol. 123, no. 1-2, pp. 395–421, 2000.
[38] J. De Geest, T. Dhaene, N. Faché and D. De Zutter, "Adaptive CAD-model building algorithm for general planar microwave structures," *IEEE Trans. Microw. Theory Tech.*, vol. 47, no. 9, pp. 1801–1809, Sep. 1999.
[39] C. P. Coelho, J. R. Phillips, and L. M. Silveira, "Passive constrained rational approximation algorithm using nevanlinna-pick interpolation," in *Proc. Design, Automation and Test in Europe Conference and Exhibition*, Mar. 4–8, 2002, pp. 923–930.
[40] E. W. Cheney, "Multivariate approximation theory: Selected topics," in *CBMS-NSF Regional Conference Series in Applied Mathematics*, vol. 51. Philadelphia, PA: SIAM, 1986.
[41] D. F. Watson, "Computing the n-dimensional delaunay tessellation with application to voronoi polytopes," *The Computer Journal*, vol. 24, no. 2, pp. 167–172, Febr. 1981.
[42] H. W. Kuhn, "Some combinatorial lemmas in topology," *IBM Journal of Research and Development*, vol. 4, no. 5, pp. 518–524, 1960.
[43] C. B. Barber, D. P. Dobkin, and H. Huhdanpaa, "The quickhull algorithm for convex hulls," *ACM Trans. Math. Softw.*, vol. 22, no. 4, pp. 469–483, 1996.
[44] D. F. Watson, *Contouring: A Guide to the Analysis and Display of Spatial Data*. Pergamon Press, 1992.
[45] S. Boyd, L. El Ghaoui, E. Feron and V. Balakrishnan, *Linear Matrix Inequalities in System and Control Theory*. Philadelphia: SIAM, 1994.
[46] M. G. Safonov, R. Y. Chiang, and D. J. N. Limebeer, "Hankel model reduction without balancing – A descriptor approach," in *Proc. 26th IEEE Conference on Decision and Control*, vol. 26, Dec. 1987, pp. 112–117.
[47] R. N. Shorten, P. Curran, K. Wulff, and E. Zeheb, "A note on spectral conditions for positive realness of transfer function matrices," *IEEE Trans. Autom. Control*, vol. 53, no. 5, pp. 1258–1261, Jun. 2008.

Francesco Ferranti received the B.S. degree (summa cum laude) in electronic engineering from the Università degli Studi di Palermo, Palermo, Italy, in 2005 and the M.S. degree (summa cum laude and honors) in electronic engineering from the Università degli Studi dell'Aquila, L'Aquila, Italy, in 2007. He is currently working towards the Ph.D. degree in the Department of Information Technology (INTEC), Ghent University, Ghent, Belgium. His research interests include parametric macromodeling, parameterized model order reduction, EMC numerical modeling, system identification.

Giulio Antonini (M'94, SM'05) received his Laurea degree (summa cum laude) in Electrical Engineering in 1994 from the Università degli Studi dell'Aquila and the Ph.D. degree in Electrical Engineering in 1998 from University of Rome "La Sapienza". Since 1998 he has been with the *UAq EMC Laboratory*, Department of Electrical Engineering of the University of L'Aquila where he is currently Associate Professor. His research interests focus on EMC analysis, numerical modeling and in the field of signal integrity for high-speed digital systems. He has authored or co-authored more than 170 technical papers and 2 book chapters. Furthermore, he has given keynote lectures and chaired several special sessions at international conferences. He has been the recipient of the IEEE Transactions on Electromagnetic Compatibility Best Paper Award in 1997, the CST University Publication Award in 2004, the IBM Shared University Research Award in 2004, 2005 and 2006, the IET-SMT Best Paper Award in 2008. In 2006 he has received a Technical Achievement Award from the IEEE EMC Society "for innovative contributions to computational electromagnetic on the Partial Element Equivalent Circuit (PEEC) technique for EMC applications". He holds one European Patent.

Tom Dhaene was born in Deinze, Belgium, on June 25, 1966. He received the Ph.D. degree in electrotechnical engineering from the University of Ghent, Ghent, Belgium, in 1993. From 1989 to 1993, he was Research Assistant at the University of Ghent, in the Department of Information Technology, where his research focused on different aspects of full-wave electro-magnetic circuit modeling, transient simulation, and time-domain characterization of high-frequency and high-speed interconnections. In 1993, he joined the EDA company Alphabit (now part of Agilent). He was one of the key developers of the planar EM simulator ADS Momentum. Since September 2000, he has been a Professor in the Department of Mathematics and Computer Science at the University of Antwerp, Antwerp, Belgium. Since October 2007, he is a Full Professor in the Department of Information Technology (INTEC) at Ghent University, Ghent, Belgium. As author or co-author, he has contributed to more than 150 peer-reviewed papers and abstracts in international conference proceedings, journals and books. He is the holder of 3 US patents.

Luc Knockaert received the M. Sc. Degree in physical engineering, the M. Sc. Degree in telecommunications engineering and the Ph. D. Degree in electrical engineering from Ghent University, Belgium, in 1974, 1977 and 1987, respectively. From 1979 to 1984 and from 1988 to 1995 he was working in North-South cooperation and development projects at the Universities of the Democratic Republic of the Congo and Burundi. He is presently affiliated with the Interdisciplinary Institute for BroadBand Technologies (www.ibbt.be) and a professor at the Dept. of Information Technology, Ghent University (www.intec.ugent.be). His current interests are the application of linear algebra and adaptive methods in signal estimation, model order reduction and computational electromagnetics. As author or co-author he has contributed to more than 100 international journal and conference publications. He is a member of MAA, SIAM and a senior member of IEEE.